

SAMRC InfoSpace

Easily accessed nitroquinolones exhibiting potent and selective antitubercular activity

Item Type	Article
Authors	Dube, P.S.;Legoabe, L.J.;Jordaan, A.;Jesumoroti, O.J.;Tshiwawa, T.;Warner, D.F.;Beteck, R.M.
Citation	Dube PS, Legoabe LJ, Jordaan A, Jesumoroti OJ, Tshiwawa T, Warner DF, Beteck RM. Easily accessed nitroquinolones exhibiting potent and selective anti-tubercular activity. Eur J Med Chem. 2021 Mar 5;213:113207. doi: 10.1016/j.ejmech.2021.113207. Epub 2021 Jan 24.
DOI	10.1016/j.ejmech.2021.113207
Publisher	Elsevier
Journal	European Journal of Medicinal Chemistry
Rights	Attribution 3.0 United States
Download date	2026-03-17 06:14:25
Item License	http://creativecommons.org/licenses/by/3.0/us/
Link to Item	https://pubmed.ncbi.nlm.nih.gov/33524688/



Easily accessed nitroquinolones exhibiting potent and selective anti-tubercular activity



Phelisiwe S. Dube^a, Lesetja J. Legoabe^a, Audrey Jordaan^b, Omobolanle J. Jesumoroti^a, Tendamudzimu Tshiwawa^c, Digby F. Warner^{b,d,e}, Richard M. Beteck^{a,*}

^a Centre of Excellence for Pharmaceutical Sciences, North-West University, Potchefstroom 2520, South Africa

^b SAMRC/NHLS/UCT Molecular Mycobacteriology Research Unit, Department of Pathology, University of Cape Town, Observatory, 7925, South Africa

^c Faculty of Science, Department of Chemistry, Rhodes University, Grahamstown 6140, South Africa

^d Institute of Infectious Disease and Molecular Medicine, University of Cape Town, Rondebosch, 7701, South Africa

^e Wellcome Centre for Infectious Diseases Research in Africa (CIDRI-Africa), Faculty of Health Sciences, University of Cape Town, Rondebosch, 7701, South Africa

ARTICLE INFO

Article history:

Received 19 August 2020

Received in revised form

24 November 2020

Accepted 12 January 2021

Available online 24 January 2021

Keywords:

Anti-tubercular

Nitro containing compounds

Quinolones

DprE1 enzyme

ABSTRACT

Nitro based DprE1 inhibitors exemplified by benzothiazinones have been reported to elicit potent anti-tubercular activity. Poor PK properties associated with benzothiazinones have inspired the discovery of alternative nitro based DprE1 inhibitors. Quinolone based antibiotics on the other hand have good PK properties. The potent anti-tubercular activity of nitro compounds and the good PK properties of the quinolones have elicited an interest in us to construct a new class of nitro containing compounds around the quinolone scaffold with the aim of identifying novel DprE1 inhibitors with potent anti-tubercular activity. Thus, we report herein the anti-tubercular activity of novel 6-nitroquinolone-3-carboxamide derivatives achieved using less than five cheap synthetic transformations. Among the 23 target compounds evaluated for anti-tubercular activity, 12 were active against Mtb— exhibiting activity in the range of <0.244–31.865 μM. Compound **25** having a molecular weight of 399 Da and ClogP value of 2.7 is the most active (MIC₉₀: <0.244 μM) in this series. The SAR analyses suggest that anti-tubercular activity was influenced by substituents at position N-1 (R₂) and C-3 (R₃) of the quinolone ring. The activity data suggest that the nature of R₃ has a stronger influence on the SAR compared to R₂; with a fluorobenzyl and chlorobenzyl moiety at R₂ being the most favoured when R₃ is an aliphatic amine. Docking study confirms that compound **25** binds to the same hydrophobic pocket as does TCA1, and other nitro based DprE1 inhibitors, with its nitro group in close proximity with Cys387 residue.

© 2021 Elsevier Masson SAS. All rights reserved.

1. Introduction

Mycobacterium tuberculosis (Mtb), the causative agent of tuberculosis (TB), is a species of pathogenic bacterium belonging to the family *Mycobacteriaceae* [1]. TB is a prehistoric disease that has been one of the major scourges of humankind since times immemorial [2]. Although Mtb has been discovered since 1882 [3], today TB still remains a major global health problem with one third of the world's population infected [4].

TB is among the top ten causes of death and the leading cause from a single pathogenic agent [5]. Globally, an estimated 10

million people fell ill with TB in 2018 and approximately 1.5 million people died from it [4,6]. The current increase in the prevalence of TB is due to noncompliance to first line TB treatment, poor efficacy of second line drugs and co-infection with HIV (Human Immunodeficiency Virus) [4,7]. Studies have shown that a close association exist between HIV infection and the development of active TB. The probability of developing active TB is higher in people living with HIV due to their compromised immune system, than in people who are HIV negative [7,8].

Worldwide in 2018, an estimated 3.4% of new cases and 18% of previously treated cases of TB were multidrug resistant (MDR-TB) and extensively drug-resistant (XDR-TB), respectively. Overall, there was an estimated 484 000 incident cases of MDR-TB and about 214 000 deaths from MDR-TB in 2018 [4]. Thus, the development of resistance to first line drugs (rifampicin, isoniazid,

* Corresponding author.

E-mail addresses: 25159194@nwu.ac.za, richmbi1@yahoo.com (R.M. Beteck).

ethambutol and pyrazinamide) by Mtb has worsened the management and treatment of TB, leading to the use of second line drugs (aminoglycosides, fluoroquinolones, thioamides, bedaquiline, and delamanid) [9]. Moreover, the emergence of MDR-TB and XDR-TB indicate not only the need for new diagnostic markers [4], drugs amendment in second line treatment regimens [10], but also emphasizes the search for new compounds exhibiting anti-tubercular activity through a mode of action that differs from currently deployed drugs [11].

Nitro containing compounds, exemplified by benzothiazinones, are new chemical entities (NCE) possessing selective and potent inhibitory activity against Mtb. They exhibit a mode of action that is completely different from other anti-tubercular agents currently in the market [12]. Most notable, this compound class have been validated to demonstrate anti-tubercular activity by acting as suicide inhibitors of Decaprenylphosphoryl- β -D-ribose 2'- epimerase (DprE1) [13]. DprE1 is a flavoprotein and a sub unit of the enzyme Decaprenylphosphoryl D-ribose (DPR) epimerase which plays a vital role in Mtb cell wall synthesis [2,14]. The discovery of DprE1 as a target of nitrobenzothiazinones (BTZs) gave an insight into these agents' mechanism of action [15] and has since inspired the investigation of other nitro-based compounds as DprE1 inhibitors and potential anti-tubercular agents [16]. In addition to BTZs, other nitro based DprE1 inhibitors reported so far includes: nitrobenzamides [17], dinitrobenzamides [18], nitroquinaxoline [19], trinitroxanthone [20], dinitrooxadiazole, dinitrotetrazole [21], dinitrothiazole [22,23], nitrotriazole [24] (see Fig. 1).

Nitro-based DprE1 inhibitors are pro-drugs activated only once inside Mtb, and hence the risk of cell toxicity is low [25]. Moreover, this class of compounds are active against drug susceptible and resistant forms of Mtb, and in some cases they show low nanomolar (~ 10 nM) activity against Mtb [2]. However, they also suffer from poor drug-like properties such as short half-life, poor aqueous solubility [25]. So far, only BTZ043 and PBTZ169 have progressed

into the early phases of clinical development [26,27]. Due to high failure rates during clinical development [28], it is pertinent to investigate other nitro-based compounds to eventually populate the development pipeline. To this effect, our group decided to investigate nitroquinolones as potential DprE1 inhibitors.

Quinolones represent an important class of organic molecules that have been known to possess broad spectrum of pharmacological properties, good pharmacokinetic properties and have attracted attention in medicinal chemistry [29,30]. Not only do they possess a wide range of pharmacological activities, they also enjoy synthetic tractability as there are several established protocols for the synthesis of this scaffold [31].

We previously identified 6-nitroquinolone-3-carboxylate ester with anti-tubercular activity as DprE1 inhibitors [32]. These compounds, however, were not soluble in screening media and were screened as suspensions. As a result, proper structure-activity relationship could not be delineated for the said compounds. In this study, we generated less lipophilic amide derivatives wherein previous compounds were substituted with polar moieties of different chain lengths and ring sizes at position C-3 of the quinolone scaffold. Analogues wherein the benzenoid ring of the quinolone template was substituted at position C-8 by either $-\text{CF}_3$, $-\text{NO}_2$, $-\text{CN}$, $-\text{F}$ where also synthesised, but only the analogue bearing $-\text{CF}_3$ (compound **3a**) was soluble in screening media and hence its data is reported herewith. All compounds in this study selected for screening were soluble in screening media.

2. Results and discussion

2.1. Chemistry

Our target compounds were obtained following a 3-step synthetic route presented in Scheme 1. The first step (a) is the condensation of diethyl ethoxymethylenemalonate (**1**) with

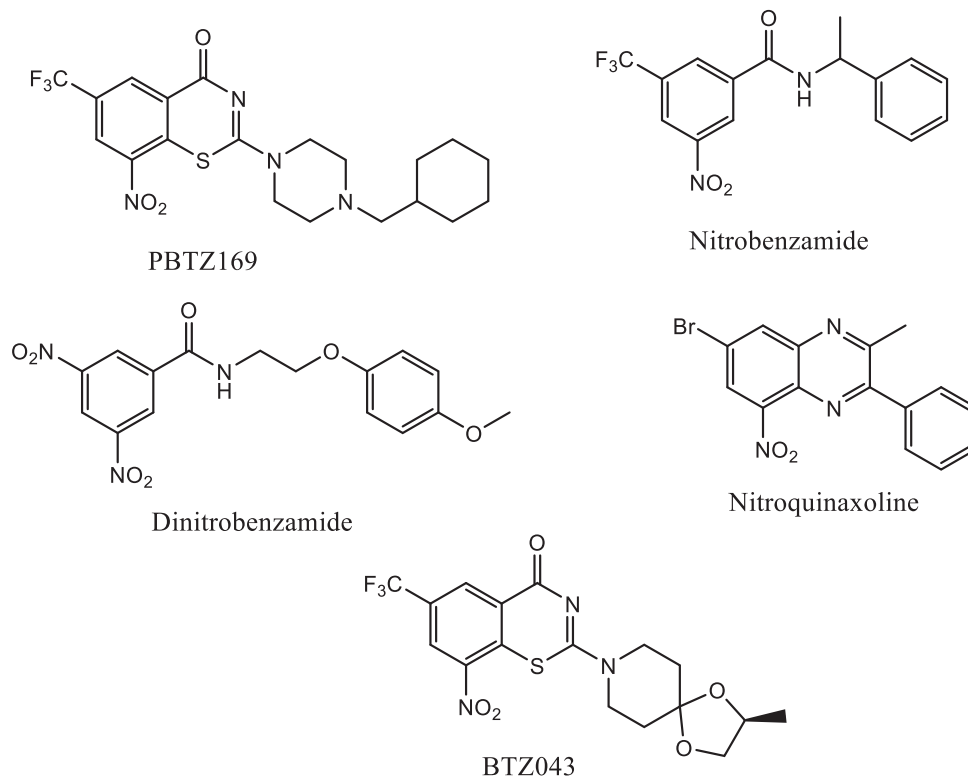


Fig. 1. Nitro containing compounds with anti-tubercular activity.

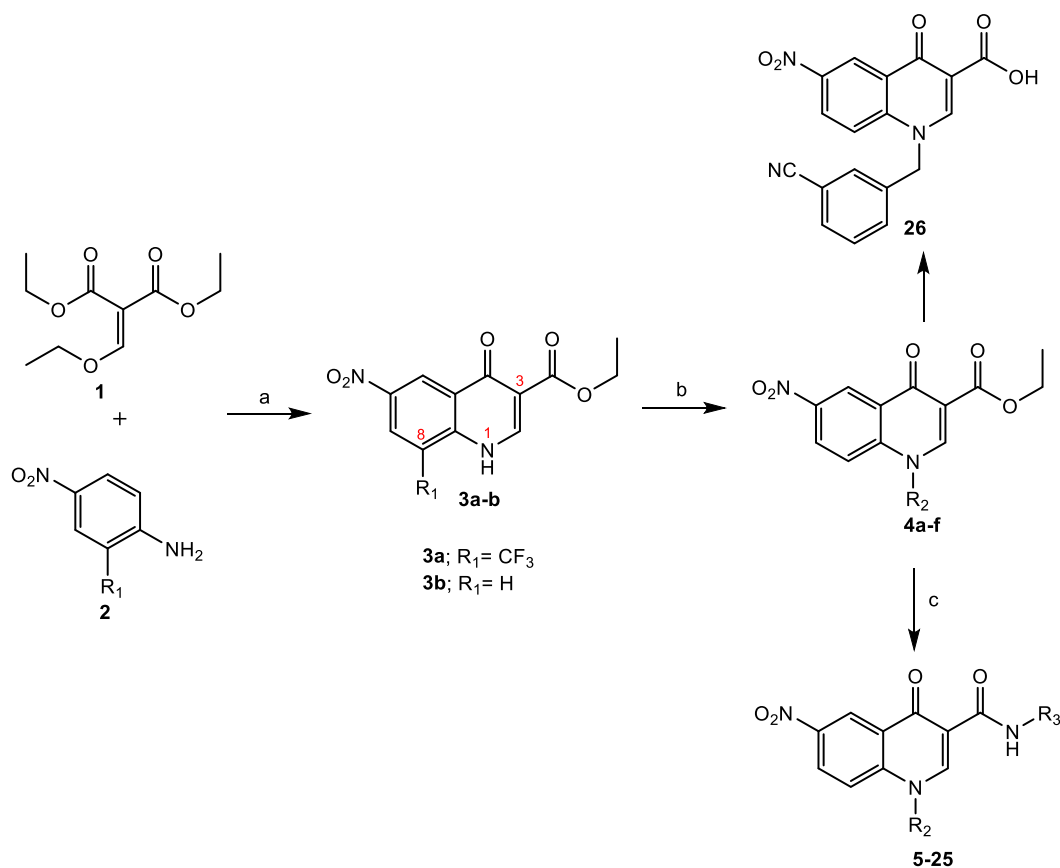
appropriate nitroaniline (**2**) followed by intramolecular cyclisation at higher temperatures of 245–250 °C to obtain intermediate **3** in 60%–90% yields. The second step (b) is the nucleophilic substitution of benzyl halides by **3b**. Intermediate **3b** was treated with potassium carbonate (K_2CO_3) to effect deprotonation of the secondary amine and enhance its nucleophilicity for subsequent nucleophilic attack of primary benzyl halides. Intermediates **4a-f** were obtained in 50%–70% yields using this step (melting points and other analytical data for these compounds are reported in ref 32). Compound **3a** and other related analogues bearing a substituent (F, CN, NO_2 , OCH_3 , CF_3) at position 8 of the quinolone ring failed to undergo nucleophilic substitution with organohalides. This could be due to steric hindrance and/or electron-withdrawing effect(s) of these substituents. In the final step (c), **4a-f** were subjected to aminolysis wherein they were treated with hydrophilic amines under reflux to obtain amide derivatives **5–25** in 50–70% overall yields. Aminolysis of **3a** using this procedure was not successful.

Reactions were monitored using thin layer chromatography (TLC) and the synthesised quinolones were characterized using 1H NMR, ^{13}C NMR, IR and high resolution mass spectrometry (HRMS). On the 1H NMR spectra, the signals of the respective protons of the prepared derivatives were verified on the basis of their chemical shifts, multiplicities and coupling constants. The signals appearing at ca 9.73–9.79 ppm of all the compounds (except **5–8**) is indicative of the presence of an amide proton ($-CONH-$). In **5–8**, the signal at ca 11.47 ppm is assignable to the OH of the hydroxamate moiety. The signal appearing at ca 5.95–6.3 ppm of all the synthesised compounds is assignable to the methylene protons of the benzyl

moiety ($Ar-CH_2-$), this is evidence of successful *N*-alkylation of the secondary amine at position N-1 by benzyl-halides. For the ^{13}C NMR spectra, the signals appearing at ca 174–176 (ketone) and 161–163 (amide) ppm of all the compounds are indicative of the two carbonyl carbons present in all compounds. The signal at ca 38–39.33 ppm of all the compounds substituted with aliphatic amines indicates the first methylene carbon of the amide moiety at R_3 . This signal is evidence of the successful conversion of an ester to an amide. This signal is absent in compound **5–8** since they contain a hydroxamate at R_3 . Lastly the signal appearing at ca 55–56 ppm of all the compounds is indicative of the methylene carbon of the benzyl moiety at R_2 and is also evidence of the successful *N*-alkylation of the secondary amine by benzyl halides. IR confirmed signature peaks corresponding to functional groups present in target molecules. HRMS analyses confirms the expected molecular ion for all compounds, except compound **8** wherein molecular ion peak not found, probably unstable with the ionization method.

2.2. Pharmacology

All target compounds (**3a**, **5–26**) were screened *in-vitro* for anti-tubercular activity against the *gfp* reporter strain of *Mtb* using middlebrook 7H9 media supplemented with casitone, glucose and tyloxpol. Rifampicin and isoniazid, a first line anti-tubercular agents were included in the assay as a reference. Target compounds were screened in a concentration range of 0.0002–10 mM and a dose – response curve generated for each compound (see ESI). The anti-tubercular activity is reported as the minimum concentration required to inhibit 90% (MIC_{90}) of bacteria population.



Scheme 1. Synthesis of target compounds^a Reagents and conditions; (a) (i) ethanol, reflux, 12 h, (ii) diphenylether, 245–250 °C, 10 min. (b) benzyl halide, DMF, K_2CO_3 , reflux, 12 h. (c) amine, reflux 24 h.

The MIC₉₀ was evaluated on day 14 following incubation of Mtb with target compounds. No precipitation was observed during screening and compounds were soluble in screening media.

The anti-tubercular activity data is summarised in Table 1. Thirteen out of the 23 compounds evaluated were active against Mtb, exhibiting activity in the range <0.244–31.865 μM. Twelve out of the 13 active compounds exhibit MIC₉₀ values < 10 μg/mL, which gives a high hit rate of >50% for this compound set.

Different substituents were appended at position N-1 (R₂) and C-3 (R₃) of the quinolone ring to enable structure-activity relationship (SAR) analysis for these series. The activity data suggest that the nature of the R₃ showed a stronger influence on the SAR than R₁. R₃ includes hydroxamate, N-(2-hydroxyethyl) ethylenediaminyl 2-methoxyethylaminyl, 2-(2-aminoethoxy) ethanolyl and 4-(2-aminoethyl) morpholinyl. With the exception of compound **10** (MIC₉₀: 31.8 μM), all compounds wherein R₃ is a hydroxamate or 4-(2-aminoethyl) morpholinyl were inactive against Mtb irrespective of the nature of R₁; for example, compound **5,7,8** and **11** were all inactive (MIC₉₀ > 125 μM). Four out of the five compounds wherein R₃ is a 2-(2-aminoethoxy)ethanolyl moiety showed anti-tubercular activity; the active compounds (**12, 14–16**) demonstrated good to moderate activity in the range of 8–16 μM. Apart from compound **19** (MIC₉₀ > 125 μM), the subseries wherein R₃ is a N-(2-hydroxyethyl)ethylenediaminyl as seen in compounds **17, 18** and **20** elicited potent anti-tubercular activity in the range of 0.9–3.7 μM R₃ in compounds **21–25** is 2-methoxyethylaminyl moiety; two compounds in this subseries exhibited sub micromolar activity, with compound **25** (MIC₉₀ < 0.244 μM) being the most active compound in this study. In compound **26** R₃ is a carboxylic acid moiety, akin to most fluoroquinolones deployed in clinics as anti-tubercular agents. This compound is, however, inactive (MIC₉₀ > 125 μM) while its amide analogues **14** (MIC₉₀: 14.9 μM) and **17** (MIC₉₀: 3.6 μM) exhibit moderate to potent anti-tubercular activity.

Overall, this study indicates that an aliphatic chain at position C-3 promotes anti-tubercular activity better than a cyclic chain or hydroxylamide at this position. This observation is evident when comparing compounds **6** (MIC₉₀; 125 μM), **10** (MIC₉₀; 31 μM), **12** (MIC₉₀; 16 μM) against compound **21** (MIC₉₀; 0.6 μM). These compounds all bear a 3-Cl-benzyl moiety as R₂, but differ Only in the nature of R₃.

The structure-activity relationship (SAR) analysis suggests that the influence of substituents at position N-1 on anti-tubercular activity depends on the substituents at position C-3 of the quinolone ring. Furthermore, the anti-tubercular activity also depends on the position (meta or para) of the groups attached to the benzyl substituent at position N-1 of quinolone core. The 4-fluorobenzyl substituted compounds showed more activity than compounds with a 3-fluorobenzyl unit substituted at position N-1. This is evident when comparing compound **13** (MIC₉₀, >125 μM) against compound **16** (MIC₉₀, 8.077 μM), **18** (MIC₉₀, 3.703 μM) against **20** (MIC₉₀ 0.919 μM), and **22** (MIC₉₀, 1.844 μM) against **25** (MIC₉₀, <0.244 μM).

Taking R₂ and R₃ together, this study suggests that R₃ substituents showing optimal anti-tubercular activity could be maintained, while R₂ could be modified further to improve on anti-tubercular activity and/or modulate other needed drug-like properties during lead development. A graphical summary of SAR analyses is presented in Fig. 2.

Compound **25** being the most active compound in this study was further evaluated *in vitro* against DprE1 mutant strain of Mtb. This compound, however, exhibited reduced activity (MIC₉₀: 62.5 μM) against DprE1 mutant compared to the wild type (MIC₉₀: <0.24 μM). This data suggests DprE1 as the likely target for compound **25**.

Table 1
In vitro anti-tubercular activity, ClogP and structure of target compounds.

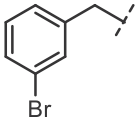
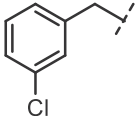
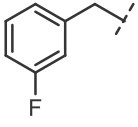
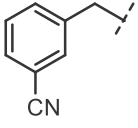
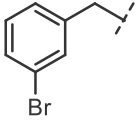
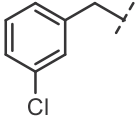
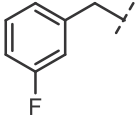
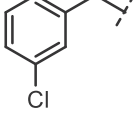
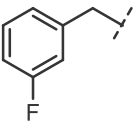
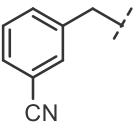
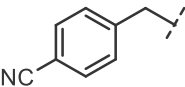
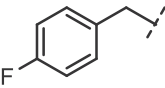
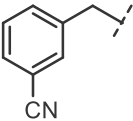
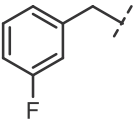
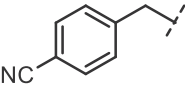
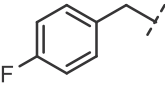
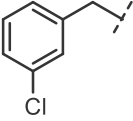
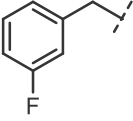
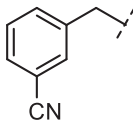
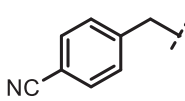
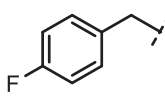
Entry	Clog P ^a	R ₂	MIC ₉₀ (μM) ^b Day 14
3a	0.72	–	1.844
5	2.67		>125
6	2.51		125
7	1.94		>125
8	1.23		>125
9	3.67		>125
10	3.51		31.865
11	2.94		>125
12	2.62		16.043

Table 1 (continued)

Entry	Clog P ^a	R ₂	MIC ₉₀ (μM) ^b Day 14
13	2.05		>125
14	1.34		14.996
15	1.34		14.01
16	2.05		8.077
17	1.18		3.687
18	1.89		3.703
19	1.18		>125
20	1.89		0.919
21	3.32		0.675
22	2.75		>125

(continued on next page)

Table 1 (continued)

Entry	Clog P ^a	R ₂	MIC ₉₀ (μM) ^b Day 14
23	2.04		>125
24	2.04		>125
25	2.75		<0.244
26	3.01	—	>125
INH	—	—	0.2
RF	—	—	0.01

^a clog P values calculated with chem draw professionals.^b MIC₉₀ = determined *in vitro* against gfp Mtb strain, RF = rifampicin, INH = isoniazid.

Compounds **3a**, **16**, **17**, **18**, **20**, **21** and **25**, all of which exhibited potent anti-tubercular activity (MIC₉₀, <10 μM) were evaluated *in vitro* against *M. ulcerans* – the causative agent for buruli ulcer. The compounds were screened in triplicate at a concentration of 10 μg/ml. *M. ulcerans* were incubated for 8 days with the compounds, then Alamar blue was added and the bacteria were incubated for another 3 days. The remaining metabolic activity (%PC) was calculated by dividing the blank-corrected fluorescence for each test compound by that of the untreated control. None of these compounds showed activity against *M. ulcerans*, all exhibiting %PC > 90%. This results evinced that these compounds have intrinsic and selective anti-tubercular activity. It is important to mention that fluoroquinolones, exemplified by ciprofloxacin, have been reported to exhibit equipotent activities against *M. tuberculosis* and *M. ulcerans* [33].

2.3. Molecular docking and theoretical drug-like properties evaluation

We previously showed that hits emanating from this compound class are not active against DprE1 mutant Mtb (ΔdprE1 C1 Tyr314His) – suggesting DprE1 as the most probable target. Based on this, we subjected compound **25** to molecular docking studies against DprE1 enzyme (PDB CODE: 4KW5). Docking confirms compound **25** binds to the hydrophobic pocket wherein other nitro based DprE1 inhibitors and TCA1 have been reported to bind [34]. Within this pocket, compound **25** makes three hydrogen bonds with the enzyme *via* LYS134, SER228 and TRP230. The ligand also made *pi-pi* interactions with the enzyme through TRY314 and TRP230 (Fig. 3a).

Unlike TCA1 which forms a non-covalent bond with CYS387 (see ESI), nitro based DprE1 inhibitors bind to the hydrophobic pocket (active site) of DprE1 enzyme and are subsequently reduced to their nitroso intermediates. The nitroso intermediate then forms a covalent adduct with a nearby CYS387. The docking pose of compound **25** within the active site of DprE1 (Fig. 3b) shows the nitro moiety of this ligand in close proximity (4.05 Å) with CYS387. This suggests that in addition to the interactions seen in Fig. 3a, compound **25** also makes covalent interaction with the enzyme. Moreover, compound **25** have a good docking score of −7.60 kcal/mol against the enzyme. All of these highlight DprE1 as the target

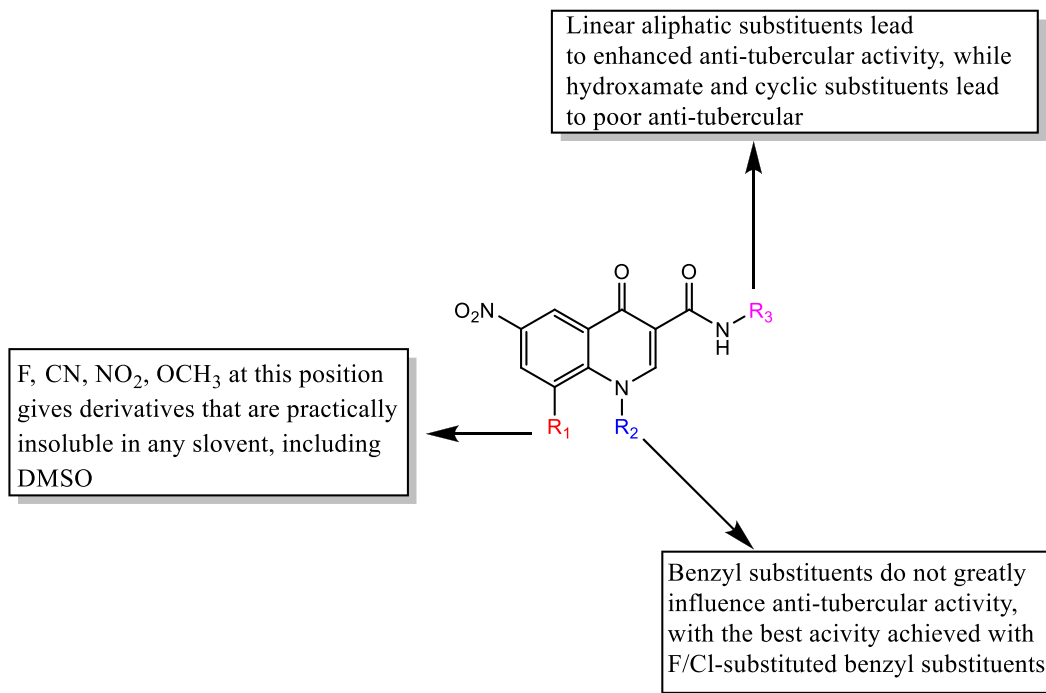


Fig. 2. Summary of property and SAR analyses of compounds investigated.

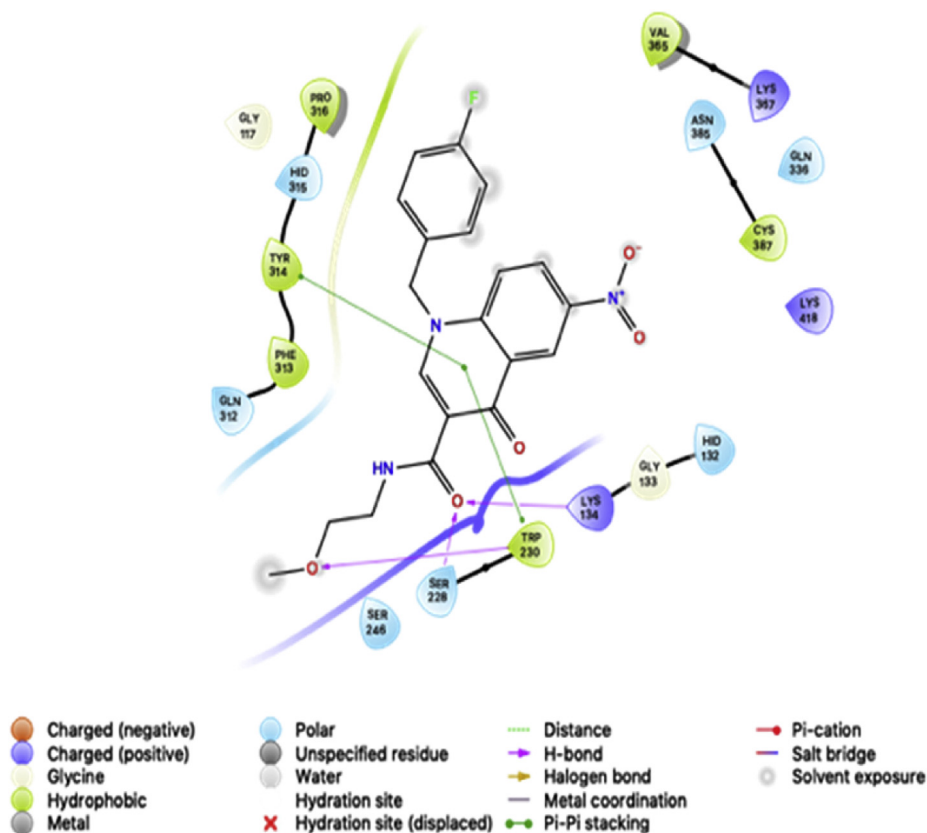


Fig. 3a. Binding interactions of compound 25 and DprE1 enzyme (PDB: 4KW5).

for compound 25.

Theoretical evaluation of the drug-likeness of the synthesised compounds suggests that the compounds are likely to possess good

physico-chemical properties. The synthesised compounds exhibited optimal lipophilicity with ClogP values ranging from 0.72 to 3.67 and were all soluble in screening media. It is noteworthy to

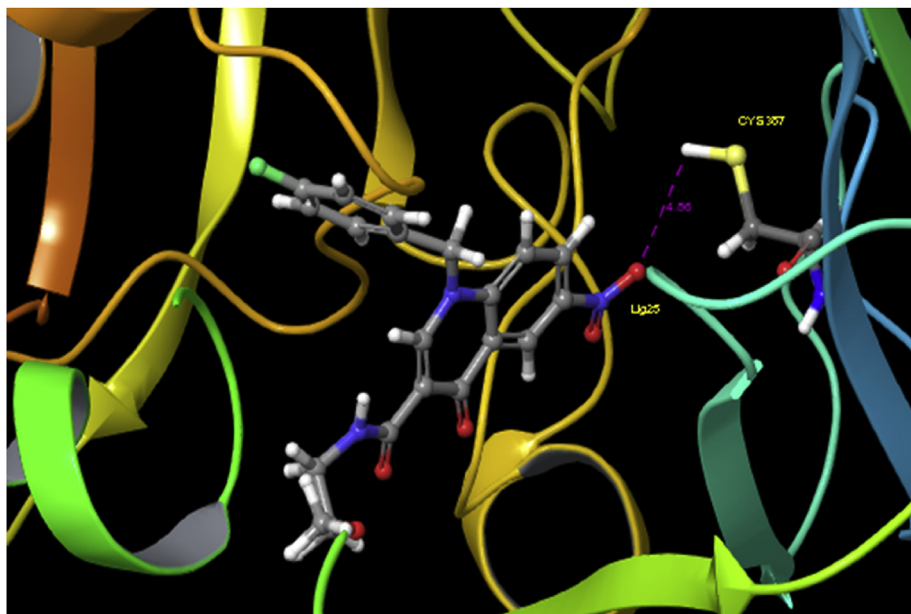


Fig. 3b. Docking pose of compound **25** in close proximity with CYS387.

mention that early *in vitro* studies have shown statistically significant improvements in safety outcomes when compounds have ClogP <3. This is a promising finding as for a long period of time, the mean value of ClogP for approved drugs has been consistent at 2.3–2.6 [35]. Moreover, the target compounds followed the Lipinski's rule of 5 with molecular weight less than 500 Da and lipophilicity expressed as ClogP less than 5 [36], giving them the potential to circumvent poor drug-like properties associated with current nitro containing anti-tubercular agents. Lipophilicity and molecular weight are often increased during hit and lead optimization. Thus, compounds with lower molecular weight and lipophilicity are more likely to maintain drug-likeness during hit and lead optimization which often involves structural incrementation [34,37].

3. Conclusion

The synthesised 6-nitroquinolone-3-carboxamides showed potent and selective anti-tubercular activity against the *gfp* strain of *Mtb*, exhibiting activity in the range of <0.244–31.865 μM . Molecular docking studies show that this compound class bind within the active pocket of DprE1 enzyme with a good docking score of -7.60 kcal/mol. The compounds are likely to possess good physico-chemical properties as they show optimal calculated lipophilicity for drug molecules, with ClogP values ranging from 0.72 to 3.67 and molecular weight <500Da. These results are encouraging and suggest that this new class of compounds is worth further exploring for potential anti-tubercular agents. The SAR highlights that the substituents at position N-1(R_2) of the quinolone ring depended on the substituents at position C-3(R_3) of the ring for anti-tubercular activity. This observation suggests that R_2 could be derivatized further to generate compounds with superior activity. Aliphatic amines at R_3 are mostly favoured. Moreover, the SAR favoured the fluorobenzyl moiety at R_2 , with the fluoride atom influencing the activity more when at para position of the benzyl unit. Compound **25** was the most active in this series ($\text{MIC}_{90} < 0.244$ μM). Furthermore, analogues of compound **3a** did not dissolve in DMSO, thus denying us structural activity analysis around the benzenoid ring of the quinolone template. **3a** showed

encouraging anti-tubercular activity (MIC_{90} 1.84 μM), low molecular weight (330 Da) and is worth further exploring.

4. Materials and methods

4.1. General information

The Chemicals and solvents used in this study were purchased from various chemical vendors: Sigma-Aldrich (Pty) Ltd. (Johannesburg, South Africa), Merck (Pty) Ltd. (Johannesburg, South Africa) and were used without purification. The progress of the reactions was monitored by thin layer chromatography (TLC) using Merck 60F254 silica gel plates (Merck, Johannesburg, South Africa) supported on aluminium and the plates were visualized under ultraviolet (UV254 and 366 nm) light or stained with iodine vapour. ^1H and ^{13}C NMR spectra were recorded on Bruker Biospin 600 MHz spectrometer, and the chemical shifts are given in values referenced to deuterated DMSO- d_6 and are reported in parts per million (ppm). Chemical shifts for deuterated DMSO- d_6 appear at 2.5 ppm for ^1H and 39.5 ppm for ^{13}C NMR spectra. Proton coupling patterns are abbreviated as follows: s (singlet), d (doublet), t (triplet), q (quartet), and m (multiplet). Coupling constants (J) are reported in Hz. NMR data were analyzed using MestReNova Software, version 5.3.2–4936. Infrared (IR) spectra were recorded using a Bruker Alpha-P FTIR instrument. Melting points (mp) were established with a Büchi melting point B-545 instrument and were uncorrected. The High-resolution mass spectra (HRMS) were recorded by means of a Bruker micrOTOF-Q II mass spectrometer using atmospheric pressure chemical ionization (APCI) in positive ion mode.

4.2. General synthetic procedure for the nitro-quinolone derivatives

Target compounds were obtained through three general procedures executed in a linear sequence as depicted in [Scheme 1](#):

- (a) To a round bottom flask containing 20 mL of ethanol, commercially available nitro-aniline was added, followed by diethylethoxymethylenemalonate (1. equiv). The flask was stirred under reflux for 12 h. After completion as indicated by

- TLC, the mixture was cooled to room temperature and the ensuing precipitate filtered, dried and later poured into boiling (250 °C) diphenylether in a 2-neck round bottom flask and heated at 245–250 °C for 10 min. The cooled mixture was washed with petroleum ether to obtain **3a–3b**.
- (b) Compound **3b** was dissolved in DMF, subsequently treated with potassium carbonate (K₂CO₃, 2. equiv), and different benzyl halides (1. equiv). The reaction mixture was stirred under reflux for 15 h. After reaction completion as indicated by TLC analysis, the reaction mixture was evaporated to dryness and deionized water poured in and stirred for 10 min. The resultant precipitate was filtered and dried to obtain compound **4a–f** in 80%–90% yields.
- (c) Target compounds 5–25 were made following the procedure reported by Beteck et al. (2019) [38]. Briefly, a gram of **4a–f** was then treated with the appropriate amine (5. equiv) in a round bottom flask containing chloroform (20 mL) followed by 1,8-diazabicyclo [5.4.0] undec-7-ene (DBU) (0.2 equiv). The resultant mixture was refluxed for 2–3 days. After reaction completion, 20 mL of chloroform was added and the mixture washed with deionized water (20 mL × 4) in a separating funnel. The organic phase was then evaporated to dryness to obtain a crude which was recrystallization from methanol to afford the corresponding target compounds **5–25** in 50–60% yields.
- (d) In to a flask containing 0.5 g (1.32 mmol) of ethyl 1-(3-cyanobenzyl)-6-nitro-4-oxo-1,4-dihydroquinolone-3-carboxylate was added 30 mL of MeOH/THF mixture (1:1 v/v), followed by LiOH (0.09 g, 3.97 mmol). The mixture was stirred at room temperature for 12 h, after which 50 mL of deionized water was added. The mixture was acidified to pH 1 by dropwise addition of concentrated HCl(aqu). The resultant precipitate was filtered, dried and recrystallized from ethanol to furnish compound **26**.

4.2.1. Ethyl 6-nitro-4-oxo-8-(trifluoromethyl)-1,4-dihydroquinolone-3-carboxylate, **3a**

Yellow powder, yield 70%, mp 236 °C. ¹H NMR (600 MHz, DMSO-*d*₆) δ 9.14 (s, 1H, Ar–H), 8.74 (s, 1H, Ar–H), 8.43 (s, 1H, Ar–H), 4.18 (q, *J* = 7.1 Hz, 2H, –OCH₂CH₃), 1.27 (t, *J* = 7.1 Hz, 3H, –OCH₂CH₃). ¹³C NMR (151 MHz, DMSO) δ 173.05, 167.04, 158.00, 152.35, 139.70, 130.36, 126.61, 124.99 (d[1]*J*_{CF} = 276 Hz), 122.09 (d[2]*J*_{CF} = 32 Hz), 110.68, 107.19, 59.14, 14.93. HRMS (*m/z*, APCI) calcd for C₁₃H₉F₃N₂O₅: 331.0408 [M+1], found: 331.0556. IR (ATR) *V*_{max} cm⁻¹: 3195.48 (N–H stretch), 3085.47 (Ar–H stretch), 2982.19 (C–H stretch), 1713.13 (C=O stretch), 1633.83 (C=O stretch).

4.2.2. 1-(3-bromobenzyl)-N-hydroxy-6-nitro-4-oxo-1,4-dihydroquinolone-3-carboxamide, **5**

Yellow powder, yield 57%, mp 236 °C. ¹H NMR (600 MHz, DMSO, *d*₆) δ 11.47 (s, 1H, OH), 9.38 (s, 1H, Ar–H), 9.16 (s, 1H, Ar–H), 9.01 (d, *J* = 2.7 Hz, 1H, Ar–H), 8.50 (dd, *J* = 9.4, 2.7 Hz, 1H, Ar–H), 7.94 (d, *J* = 9.4 Hz, 1H, Ar–H), 7.57 (s, 1H, NH), 7.51 (d, *J* = 8.0 Hz, 1H, Ar–H), 7.30 (t, *J* = 7.9 Hz, 1H, Ar–H), 7.19 (d, *J* = 7.8 Hz, 1H, Ar–H), 5.87 (s, 2H, Ar–CH₂). ¹³C NMR (151 MHz, DMSO, *d*₆) δ 174.05, 160.91, 149.48, 143.48, 142.13, 137.69, 130.67, 130.52, 128.98, 126.52, 126.29, 124.98, 121.83, 121.78, 119.38, 112.17, 55.05. HRMS (*m/z*, APCI) calcd for C₁₇H₁₂BrN₃O₅: 418.0033 [M+1], found: 418.0026. IR (ATR) *V*_{max} cm⁻¹: 3205.91 (O–H stretch), 3083.7 (Ar–H stretch), 2900.78 (C–H stretch), 1653.73 (C=O stretch), 1603.99 (C=O stretch).

4.2.3. 1-(3-chlorobenzyl)-N-hydroxy-6-nitro-4-oxo-1,4-dihydroquinolone-3-carboxamide, **6**

Yellow powder, yield 59%, mp 263–265 °C. ¹H NMR (600 MHz,

DMSO, *d*₆) δ 11.47 (s, 1H, OH), 9.37 (s, 1H, Ar–H), 9.17 (s, 1H, Ar–H), 9.02 (d, *J* = 2.7 Hz, 1H, Ar–H), 8.50 (dd, *J* = 9.4, 2.7 Hz, 1H, Ar–H), 7.94 (d, *J* = 9.4 Hz, 1H, Ar–H), 7.42 (s, 1H, NH), 7.39–7.35 (m, 2H, Ar–H), 7.16 (d, *J* = 6.3 Hz, 1H, Ar–H), 5.87 (s, 2H, CH₂). ¹³C NMR (151 MHz, DMSO, *d*₆) δ 174.78, 161.64, 150.22, 144.21, 142.87, 138.20, 133.86, 131.14, 128.33, 127.24, 127.03, 126.85, 125.35, 122.56, 120.12, 112.90, 55.86. HRMS (*m/z*, APCI) calcd for C₁₇H₁₂ClN₃O₅: 374.0490 [M+1], found: 374.0490. IR (ATR) *V*_{max} cm⁻¹: 3215.14 (O–H stretch), 3056.31 (Ar–H stretch), 1650.97 (C=O stretch), 1601.63 (C=O stretch).

4.2.4. 1-(3-fluorobenzyl)-N-hydroxy-6-nitro-4-oxo-1,4-dihydroquinolone-3-carboxamide, **7**

Yellow powder, yield 61%, mp 245–246 °C. ¹H NMR (600 MHz, DMSO, *d*₆) δ 11.47 (s, 1H, OH), 9.38 (s, 1H, Ar–H), 9.17 (s, 1H, Ar–H), 9.00 (dd, *J* = 14.5, 2.7 Hz, 1H, Ar–H), 8.49 (dd, *J* = 9.4, 2.7 Hz, 1H, Ar–H), 7.93 (d, *J* = 9.4 Hz, 1H, Ar–H), 7.43–7.36 (m, 1H, Ar–H), 7.19–7.11 (m, 2H, Ar–H, NH), 7.05 (d, *J* = 7.8 Hz, 1H, Ar–H), 5.85 (d, *J* = 38.9 Hz, 2H, Ar–CH₂). ¹³C NMR (151 MHz, DMSO, *d*₆) δ 174.37, 161.39 (¹*J*_{CF} = 244 Hz), 161.22, 149.79, 143.77, 142.48, 138.12 (²*J*_{CF} = 15 Hz), 130.94 (³*J*_{CF} = 8.2 Hz), 126.78 (⁴*J*_{CF} = 26 Hz), 122.31, 122.13, 119.73, 114.83 (⁵*J*_{CF} = 7.2 Hz), 113.62, 113.47, 112.49, 55.57. HRMS (*m/z*, APCI) calcd for C₁₇H₁₂FN₃O₅: 358.0834 [M+1], found: 358.0838. IR (ATR) *V*_{max} cm⁻¹: 3224.49 (O–H stretch), 3056.47 (Ar–H stretch), 1772.84 (C=O stretch), 1655.58 (C=O stretch).

4.2.5. 1-(3-cyanobenzyl)-N-hydroxy-6-nitro-4-oxo-1,4-dihydroquinolone-3-carboxamide, **8**

Yellow powder, yield 50%, mp 250 °C. ¹H NMR (600 MHz, DMSO, *d*₆) δ 11.49 (s, 1H, OH), 9.66 (s, 1H, Ar–H), 9.20 (s, 1H, Ar–H), 9.02 (d, *J* = 2.7 Hz, 1H, Ar–H), 8.48 (dd, *J* = 9.4, 2.7 Hz, 1H, Ar–H), 7.94 (d, *J* = 9.4 Hz, 1H, Ar–H), 7.59 (d, *J* = 7.8 Hz, 1H, Ar–H), 7.51 (s, 1H, NH), 7.38 (t, *J* = 7.7 Hz, 1H, Ar–H), 7.31 (d, *J* = 7.8 Hz, 1H, Ar–H), 5.80 (s, 2H, CH₂). ¹³C NMR (151 MHz, DMSO, *d*₆) δ 174.06, 161.00, 149.92, 149.65, 143.52, 142.20, 134.90, 133.59, 128.44, 126.72, 126.48, 126.30, 124.66, 122.75, 121.85, 119.61, 112.00, 55.92. HRMS: molecular ion peak not found, probably unstable with the ionization method. IR (ATR) *V*_{max} cm⁻¹: 3370.35 (O–H stretch), 3038.80 (Ar–H stretch), 2957.52 (C–H stretch), 1653.70 (C=O stretch), 1602.93 (C=O stretch).

4.2.6. 1-(3-bromobenzyl)-N-(2-morpholinoethyl)-6-nitro-4-oxo-1,4-dihydroquinolone-3-carboxamide, **9**

Mustard powder, yield 55%, mp 50 °C. ¹H NMR (600 MHz, DMSO, *d*₆) δ 9.79 (t, *J* = 5.2 Hz, 1H, NH), 9.15 (s, 1H, Ar–H), 9.04 (d, *J* = 2.4 Hz, 1H, Ar–H), 8.49 (dd, *J* = 9.3, 2.4 Hz, 1H, Ar–H), 7.93 (d, *J* = 9.3 Hz, 1H, Ar–H), 7.57 (s, 1H, Ar–H), 7.53 (d, *J* = 8.0 Hz, 1H, Ar–H), 7.31 (t, *J* = 7.8 Hz, 1H, Ar–H), 7.19 (d, *J* = 7.7 Hz, 1H, Ar–H), 5.85 (s, 2H, Ar–CH₂), 3.65–3.60 (m, 4H, 2 × CH₂), 3.49 (dd, *J* = 11.9, 6.0 Hz, 3H, morpholinyl–H), 2.45 (s, 5H, morpholinyl–H). ¹³C NMR (151 MHz, DMSO, *d*₆) δ 175.16, 162.65, 149.88, 143.42, 142.30, 137.67, 130.57, 130.49, 128.98, 126.71, 126.37, 124.99, 121.74, 121.68, 119.27, 112.53, 65.80, 56.67, 54.96, 52.73, 35.27. HRMS (*m/z*, APCI) calcd for C₂₃H₂₃BrN₄O₅: 515.0925 [M+1], found: 515.0924. IR (ATR) *V*_{max} cm⁻¹: 3240.18 (N–H stretch), 3080.37 (Ar–H stretch), 2957.76 (C–H stretch), 1698.05 (C=O stretch), 1683.20 (C=O stretch).

4.2.7. 1-(3-chlorobenzyl)-N-(2-morpholinoethyl)-6-nitro-4-oxo-1,4-dihydroquinolone-3-carboxamide, **10**

Yellow powder, yield 54%, mp 243–245 °C. ¹H NMR (600 MHz, DMSO, *d*₆) δ 9.77 (t, *J* = 5.3 Hz, 1H, NH), 9.14 (s, 1H, Ar–H), 9.04 (d, *J* = 3.5 Hz, 1H, Ar–H), 8.52–8.46 (m, 1H, Ar–H), 7.94 (d, *J* = 9.0 Hz, 1H, Ar–H), 7.42 (s, 1H, Ar–H), 7.39–7.34 (m, 2H, Ar–H), 7.16 (d, *J* = 4.2 Hz, 1H, Ar–H), 5.85 (s, 2H, Ar–CH₂), 3.62 (t, *J* = 4.3 Hz, 4H,

2 × CH₂), 3.49 (dd, *J* = 11.9, 6.0 Hz, 3H, morpholinyl-H), 2.45 (s, 5H, morpholinyl-H). ¹³C NMR (151 MHz, DMSO, *d*₆) δ 174.76, 162.61, 149.91, 143.47, 142.27, 137.45, 133.15, 130.42, 127.61, 126.72, 126.40, 126.14, 124.66, 121.81, 119.29, 112.51, 65.83, 56.69, 55.07, 52.75, 35.29. HRMS (*m/z*, APCI) calcd for C₂₃H₂₃ClN₄O₅: 471.1430 [M+1], found: 471.1425. IR (ATR) *V*_{max} cm⁻¹: 3244.81(N-H stretch), 3080.55(Ar-H stretch), 2959.06(C-H stretch), 1656.22(C=O stretch), 1610.88(C=O stretch).

4.2.8. 1-(3-fluorobenzyl)-N-(2-morpholinoethyl)-6-nitro-4-oxo-1,4-dihydroquinolone-3-carboxamide, 11

Yellow powder, yield 60%, mp 246 °C. ¹H NMR (600 MHz, DMSO, *d*₆) δ 9.76 (t, *J* = 5.3 Hz, 1H, NH), 9.13 (s, 1H, Ar-H), 9.03 (d, *J* = 2.3 Hz, 1H, Ar-H), 8.48 (dd, *J* = 9.3, 2.3 Hz, 1H, Ar-H), 7.93 (d, *J* = 9.3 Hz, 1H, Ar-H), 7.39 (dd, *J* = 3.3, 7.7 Hz, 1H, Ar-H), 7.15 (dd, *J* = 8.5, 9.4 Hz, 2H, Ar-H), 7.05 (d, *J* = 7.7 Hz, 1H, Ar-H), 5.86 (s, 2H, Ar-CH₂), 3.62 (t, *J* = 4.3 Hz, 4H, 2 × CH₂), 3.49 (q, *J* = 6.0 Hz, 3H, morpholinyl-H), 2.44 (s, 5H, morpholinyl-H). ¹³C NMR (151 MHz, DMSO, *d*₆) δ 175.69, 163.56 (¹*J*_{CF} = 244.0 Hz), 162.03, 150.85, 144.37, 143.25, 138.77, 138.72, 131.57 (³*J*_{CF} = 8.5 Hz), 127.48 (²*J*_{CF} = 56.3 Hz), 122.98 (⁴*J*_{CF} = 3.0 Hz), 122.74, 120.26, 115.39 (²*J*_{CF} = 21.1 Hz), 114.19 (³*J*_{CF} = 22.2 Hz), 113.49, 66.77, 57.64, 56.13, 53.69, 36.23. HRMS (*m/z*, APCI) calcd for C₂₃H₂₃FN₄O₅: 455.1725 [M+1], found: 455.1724. IR (ATR) *V*_{max} cm⁻¹: 3234.51(N-H stretch), 3054.69(Ar-H stretch), 2921.24(C-H stretch), 1655.36(C=O stretch), 1610.45(C=O stretch).

4.2.9. 1-(3-chlorobenzyl)-N-(2-(2-hydroxyethoxy) ethyl)-6-nitro-4-oxo-1,4-dihydroquinolone-3-carboxamide, 12

Mustard powder, yield 50%, mp 50 °C. ¹H NMR (600 MHz, DMSO, *d*₆) δ 10.19 (t, *J* = 5.3 Hz, 1H, NH), 9.56 (s, 1H, Ar-H), 9.45 (d, *J* = 2.5 Hz, 1H, Ar-H), 8.91 (dd, *J* = 9.4, 2.5 Hz, 1H, Ar-H), 8.36 (d, *J* = 9.4 Hz, 1H, Ar-H), 7.80 (dd, *J* = 9.9, 4.3 Hz, 3H, Ar-H), 7.58 (d, *J* = 4.0 Hz, 1H, Ar-H), 6.27 (s, 2H, Ar-CH₂), 5.00 (t, *J* = 5.4 Hz, 1H, OH), 4.02–3.89 (m, 9H, NH, 4 × CH₂). ¹³C NMR (151 MHz, DMSO, *d*₆) δ 175.72, 163.70, 150.93, 144.42, 143.22, 138.38, 134.10, 131.36, 128.55, 127.64, 127.37, 127.10, 125.60, 122.72, 120.27, 113.37, 72.68, 69.65, 60.74, 56.05, 39.17. HRMS (*m/z*, APCI) calcd for C₂₁H₂₀ClN₄O₅: 446.1113 [M+1], found: 446.1076. IR (ATR) *V*_{max} cm⁻¹: 3206.72(N-H stretch), 3040.02(Ar-H stretch), 2893.26(C-H stretch), 1716.78(C=O stretch), 1698.40(C=O stretch).

4.2.10. 1-(3-fluorobenzyl)-N-(2-(2-hydroxyethoxy) ethyl)-6-nitro-4-oxo-1,4-dihydroquinolone-3-carboxamide, 13

Yellow powder, yield 52%, mp 198–200 °C. ¹H NMR (600 MHz, DMSO, *d*₆) δ 9.76 (t, *J* = 5.5 Hz, 1H, NH), 9.13 (s, 1H, Ar-H), 9.00 (d, *J* = 2.8 Hz, 1H, Ar-H), 8.46 (dd, *J* = 9.4, 2.8 Hz, 1H, Ar-H), 7.91 (d, *J* = 9.4 Hz, 1H, Ar-H), 7.40–7.35 (m, 1H, Ar-H), 7.18–7.09 (m, 2H, Ar-H), 7.03 (d, *J* = 7.8 Hz, 1H, Ar-H), 5.85 (s, 2H, Ar-CH₂), 4.60 (t, *J* = 5.2 Hz, 1H, OH), 3.57–3.45 (m, 8H, 4 × CH₂). ¹³C NMR (151 MHz, DMSO, *d*₆) δ 175.50, 163.84 (¹*J*_{CF} = 244 Hz), 161.80, 150.74, 144.17, 143.39, 138.90 (²*J*_{CF} = 25 Hz), 131.74 (³*J*_{CF} = 8.3 Hz), 127.79 (³*J*_{CF} = 8 Hz), 123.12, 122.87, 120.48, 115.63, 115.49, 114.43 (⁴*J*_{CF} = 5 Hz), 113.48, 72.85, 69.82, 60.89, 56.32, 39.33. HRMS (*m/z*, APCI) calcd for C₂₁H₂₀FN₄O₆: 430.1409 [M+1], found: 430.1373. IR (ATR) *V*_{max} cm⁻¹: 3384.88(O-H stretch), 3195.40(N-H stretch), 3059.15(Ar-H stretch), 2916.73(C-H stretch), 1659.41(C=O stretch), 1610.81(C=O stretch).

4.2.11. 1-(cyanobenzyl)-N-(2-(hydroxyethoxy) ethyl)-6-nitro-4-oxo-1,4-dihydroquinolone-3-carboxamide, 14

Mustard powder, yield 55%, mp 234 °C. ¹H NMR (600 MHz, DMSO, *d*₆) δ 9.79 (t, *J* = 5.4 Hz, 1H, NH), 9.16 (s, 1H, Ar-H), 9.02 (d, *J* = 4.3 Hz, 1H, Ar-H), 8.47 (dd, *J* = 9.4, 4.3 Hz, 1H, Ar-H), 7.88 (t, *J* = 11.5 Hz, 1H, Ar-H), 7.83 (s, 1H, Ar-H), 7.78 (dd, *J* = 7.9, 6.5 Hz,

1H, Ar-H), 7.62–7.48 (m, 2H, Ar-H), 5.90 (s, 2H, Ar-CH₂), 4.62 (t, *J* = 5.4 Hz, 1H, OH), 3.62–3.44 (m, 8H, 4 × CH₂). ¹³C NMR (151 MHz, DMSO, *d*₆) δ 175.18, 163.09, 150.45, 143.72, 142.54, 136.95, 131.71, 131.20, 130.16, 129.99, 127.10, 126.74, 122.06, 119.61, 118.27, 112.82, 111.74, 72.05, 69.03, 60.09, 55.35, 38.52. HRMS (*m/z*, APCI) calcd for C₂₂H₂₀N₄O₆: 437.1456 [M+1], found: 437.1422. IR (ATR) *V*_{max} cm⁻¹: 3190.88(O-H stretch), 3057.57(Ar-H stretch), 2929.13(C-H stretch), 2227.07(C≡N stretch), 1654.99(C=O stretch), 1608.84(C=O stretch).

4.2.12. 1-(4-cyanobenzyl)-N-(2-(2-hydroxyethoxy) ethyl)-6-nitro-4-oxo-1,4-dihydroquinolone-3-carboxamide, 15

Mustard powder, yield 53%, mp 240–242 °C. ¹H NMR (600 MHz, DMSO, *d*₆) δ 9.74 (t, *J* = 5.5 Hz, 1H, NH), 9.14 (s, 1H, Ar-H), 9.04 (d, *J* = 2.7 Hz, 1H, Ar-H), 8.46 (dd, *J* = 9.4, 2.7 Hz, 1H, Ar-H), 7.87 (d, *J* = 9.4 Hz, 1H, Ar-H), 7.83–7.80 (m, 2H, Ar-H), 7.44 (d, *J* = 8.4 Hz, 2H, Ar-H), 5.95 (s, 2H, Ar-CH₂), 4.51 (s, 1H, OH), 3.60 (t, *J* = 5.6 Hz, 2H, CH₂), 3.54 (dd, *J* = 7.8, 5.3 Hz, 4H, 2 × CH₂), 3.50 (dd, *J* = 5.5, 5.6 Hz, 2H, CH₂). ¹³C NMR (151 MHz, DMSO, *d*₆) δ 174.81, 162.73, 150.09, 143.56, 142.32, 140.62, 132.38, 127.04, 126.77, 126.43, 121.83, 119.28, 117.94, 112.66, 110.43, 71.79, 68.76, 59.88, 55.38, 39.30. HRMS (*m/z*, APCI) calcd for C₂₂H₂₀N₄O₆: 437.1456 [M+1], found: 437.1416. IR (ATR) *V*_{max} cm⁻¹: 3525.44(O-H stretch), 3245.71(N-H stretch), 3055.31(Ar-H stretch), 2864.73(C-H stretch), 2228.30(C≡N stretch), 1655.37(C=O stretch), 1609.55(C=O stretch).

4.2.13. 1-(4-fluorobenzyl)-N-(2-(2-hydroxyethoxy) ethyl)-6-nitro-4-oxo-1,4-dihydroquinolone-3-carboxamide, 16

Yellow powder, yield 55%, mp 193–194 °C. ¹H NMR (600 MHz, DMSO, *d*₆) δ 9.78 (t, *J* = 5.5 Hz, 1H, NH), 9.15 (s, 1H, Ar-H), 9.02 (d, *J* = 2.7 Hz, 1H, Ar-H), 8.48 (dd, *J* = 9.4, 2.7 Hz, 1H, Ar-H), 7.98 (d, *J* = 9.4 Hz, 1H, Ar-H), 7.34 (dd, *J* = 8.6, 5.4 Hz, 2H, Ar-H), 7.19 (t, *J* = 8.8 Hz, 2H, Ar-H), 5.83 (s, 2H, Ar-CH₂), 4.61 (t, *J* = 5.4 Hz, 1H, OH), 3.60–3.47 (m, 8H, 4 × CH₂). ¹³C NMR (151 MHz, DMSO, *d*₆) δ 175.80, 163.86 (¹*J*_{CF} = 240 Hz), 161.59, 150.97, 144.53, 143.35, 132.17 (⁴*J*_{CF} = 3.0 Hz), 129.56 (³*J*_{CF} = 8.3 Hz), 127.77, 127.45, 116.47 (²*J*_{CF} = 21.7 Hz), 116.54, 116.40, 113.41, 72.85, 69.82, 60.89, 56.13, 39.32. HRMS (*m/z*, APCI) calcd for C₂₁H₂₀FN₄O₆: 430.1409 [M+1], found: 430.1389. IR (ATR) *V*_{max} cm⁻¹: 3403.74(O-H stretch), 3299.53(N-H stretch), 3042.47(Ar-H stretch), 2890.23(C-H stretch), 1660.78(C=O stretch), 1610.17(C=O stretch).

4.2.14. 1-(3-cyanobenzyl)-N-(2-(2-hydroxyethyl) amino) ethyl)-6-nitro-4-oxo-1,4-dihydroquinolone-3-carboxamide, 17

Mustard powder, yield 50%, mp 51 °C. ¹H NMR (600 MHz, DMSO, *d*₆) δ 9.76 (d, *J* = 5.5 Hz, 1H, NH), 9.14–9.01 (m, 2H, Ar-H), 8.47 (d, *J* = 7.5 Hz, 1H, Ar-H), 7.84 (dd, *J* = 7.5, 8.4 Hz, 3H, Ar-H), 7.57 (s, 2H, Ar-H), 5.89 (s, 2H, Ar-CH₂), 4.49 (s, 1H, OH), 3.46 (d, *J* = 4.5 Hz, 2H, CH₂), 3.43 (d, *J* = 4.5 Hz, 2H, CH₂), 2.73 (s, 2H, CH₂), 2.63 (s, 2H, CH₂). ¹³C NMR (151 MHz, DMSO, *d*₆) δ 175.16, 163.02, 150.36, 143.71, 142.55, 136.98, 131.74, 131.23, 130.18, 130.02, 127.11, 126.72, 122.09, 119.59, 118.30, 113.02, 111.77, 60.29, 55.35, 51.32, 48.43, 39.80. HRMS (*m/z*, APCI) calcd for C₂₂H₂₁N₅O₅: 436.1615 [M+1], found: 436.1609. IR (ATR) *V*_{max} cm⁻¹: 3226.80(O-H stretch), 3046.23(Ar-H stretch), 2839.12(C-H stretch), 2225.26(C≡N stretch), 1654.25(C=O stretch), 1608.51(C=O stretch).

4.2.15. 1-(3-fluorobenzyl)-N-(2-(2-hydroxyethyl) amino) ethyl)-6-nitro-4-oxo-1,4-dihydroquinolone-3-carboxamide, 18

Mustard powder, yield 51%, mp 191 °C. ¹H NMR (600 MHz, DMSO, *d*₆) δ 9.75 (t, *J* = 5.5 Hz, 1H, NH), 9.14 (s, 1H, Ar-H), 9.01 (d, *J* = 2.7 Hz, 1H, Ar-H), 8.48 (dd, *J* = 9.4, 2.7 Hz, 1H, Ar-H), 7.93 (t, *J* = 10.0 Hz, 1H, Ar-H), 7.39 (td, *J* = 8.0, 6.3 Hz, 1H, Ar-H), 7.20–7.10 (m, 2H, Ar-H), 7.05 (t, *J* = 8.1 Hz, 1H, Ar-H), 5.85 (s, 2H, Ar-CH₂),

4.47 (s, 1H, OH), 3.50–3.40 (m, 5H, NH, 2 × CH₂), 2.75–2.60 (m, 4H, 2 × CH₂). ¹³C NMR (151 MHz, DMSO, d₆) δ 175.03, 162.99 (¹J_{CF} = 239 Hz), 161.39, 150.23, 143.71, 142.59, 138.12 (³J_{CF} = 15 Hz), 130.95 (³J_{CF} = 8.4 Hz), 126.98 (⁴J_{CF} = 4.4 Hz), 122.32, 122.08, 119.64, 114.83 (²J_{CF} = 25 Hz), 114.69, 113.63 (²J_{CF} = 25 Hz), 112.88, 60.28, 55.50, 51.32, 48.41, 38.82. HRMS (m/z, APCI) calcd for C₂₁H₂₁FN₄O₅: 429.1569 [M+1], found: 429.1569. IR (ATR) V_{max} cm⁻¹: 3244.57(O–H stretch), 3054.94(Ar–H stretch), 2840.71(C–H stretch), 1658.89(C=O stretch), 1612.45(C=O stretch).

4.2.16. 1-(4-cyanobenzyl)-N-(2-(2-hydroxyethyl) amino) ethyl)-6-nitro-4-oxo-1,4-dihydroquinolone-3-carboxamide, 19

Yellow powder, yield 61%, mp 238–239 °C. ¹H NMR (600 MHz, DMSO, d₆) δ 9.71 (t, J = 5.5 Hz, 1H, NH), 9.16–9.11 (m, 1H, Ar–H), 9.04 (t, J = 5.8 Hz, 1H, Ar–H), 8.45 (dd, J = 9.4, 2.8 Hz, 1H, Ar–H), 7.87 (dd, J = 9.4, 5.5 Hz, 1H, Ar–H), 7.81 (d, J = 8.4 Hz, 2H, Ar–H), 7.44 (t, J = 8.0 Hz, 2H, Ar–H), 5.94 (s, 2H, Ar–CH₂), 4.36 (s, 1H, OH), 3.52–3.37 (m, 5H, NH, 2 × CH₂), 2.77–2.73 (m, 2H, CH₂), 2.67–2.62 (m, 2H, CH₂). ¹³C NMR (151 MHz, DMSO, d₆) δ 175.06, 162.91, 150.28, 143.82, 142.60, 140.93, 132.66, 127.32, 127.05, 126.68, 122.12, 118.22, 113.13, 110.71, 60.35, 55.65, 51.32, 48.42, 38.91. HRMS (m/z, APCI) calcd for C₂₂H₂₁N₅O₅: 436.1615 [M+1], found: 436.1625. IR (ATR) V_{max} cm⁻¹: 3220.88 (O–H stretch), 3047.22(Ar–H stretch), 2836.25(C–H stretch), 2228.99(C≡N stretch), 1658.05(C=O stretch).

4.2.17. 1-(4-fluorobenzyl)-N-(2-(2-hydroxyethyl) amino) ethyl)-6-nitro-4-oxo-1,4-dihydroquinolone-3-carboxamide, 20

Yellow powder, yield 50% mp 50 °C. ¹H NMR (600 MHz, DMSO, d₆) δ 9.75 (s, 1H, NH), 9.14 (s, 1H, Ar–H), 9.02 (s, 1H, Ar–H), 8.48 (d, J = 9.2 Hz, 1H, Ar–H), 7.97 (d, J = 9.3 Hz, 1H, Ar–H), 7.33 (s, 2H, Ar–H), 7.19 (t, J = 8.3 Hz, 2H, Ar–H), 5.83 (s, 2H, Ar–CH₂), 4.47 (s, 1H, OH), 3.50–3.40 (m, 5H, NH, 2 × CH₂), 2.87–2.62 (m, 4H, 2 × CH₂). ¹³C NMR (151 MHz, DMSO, d₆) δ 174.96, 162.94, 150.08 (¹J_{CF} = 244 Hz), 143.69, 142.54, 131.06, 128.75 (³J_{CF} = 8.0 Hz), 126.97, 126.61 (⁴J_{CF} = 3.8 Hz), 122.06, 119.72, 115.74 (²J_{CF} = 15 Hz), 115.60, 112.81, 60.27, 55.30, 51.31, 48.40, 38.81. HRMS (m/z, APCI) calcd for C₂₁H₂₁FN₄O₅: 429.1569 [M+1], found: 429.1590. IR (ATR) V_{max} cm⁻¹: 3205.68 (N–H stretch), 3043.47(Ar–H stretch), 2918.49(C–H stretch), 1655.96(C=O stretch), 1610.71(C=O stretch).

4.2.18. 1-(3-chlorobenzyl)-N-(2-methoxyethyl)-6-nitro-4-oxo-1,4-dihydroquinolone-3-carboxamide, 21

Mustard powder, yield 60% mp 194–196 °C. ¹H NMR (600 MHz, DMSO, d₆) δ 9.78 (t, J = 5.3 Hz, 1H, NH), 9.15 (s, 1H, Ar–H), 9.01 (t, J = 5.3 Hz, 1H, Ar–H), 8.49 (dd, J = 9.4, 2.8 Hz, 1H, Ar–H), 7.93 (d, J = 9.4 Hz, 1H, Ar–H), 7.45–7.33 (m, 3H, Ar–H), 7.15 (dd, J = 7.6, 4.9 Hz, 1H, Ar–H), 5.86 (s, 2H, Ar–CH₂), 3.59–3.46 (m, 4H, 2 × CH₂), 3.31 (s, 3H, CH₃). ¹³C NMR (151 MHz, DMSO, d₆) δ 175.72, 163.67, 150.96, 144.35, 143.19, 138.40, 134.11, 131.36, 128.54, 127.61, 127.39, 127.08, 125.57, 122.71, 120.28, 113.29, 71.17, 58.24, 55.94, 38.87. HRMS (m/z, APCI) calcd for C₂₀H₁₈ClN₃O₅: 416.1008 [M+1], found: 416.1028. IR (ATR) V_{max} cm⁻¹: 3084.41(Ar–H stretch), 2879.66(C–H stretch), 1656.23(C=O stretch), 1610.60(C=O stretch).

4.2.19. 1-(3-fluorobenzyl)-N-(2-methoxyethyl) 6-nitro-4-oxo-1,4-dihydroquinolone-3-carboxamide, 22

Yellow powder, yield 65% mp 237–239 °C. ¹H NMR (600 MHz, DMSO, d₆) δ 9.78 (t, J = 5.1 Hz, 1H, NH), 9.14 (d, J = 4.6 Hz, 1H, Ar–H), 9.02 (d, J = 2.5 Hz, 1H, Ar–H), 8.48 (dd, J = 9.3, 2.5 Hz, 1H, Ar–H), 7.90 (dd, J = 2.5, 9.4 Hz, 1H, Ar–H), 7.39 (dd, J = 10.2, 7.7 Hz, 1H, Ar–H), 7.22–7.09 (m, 2H, Ar–H), 7.05 (d, J = 7.7 Hz, 1H, Ar–H), 5.87 (s, 2H, Ar–CH₂), 3.51 (dt, J = 7.0, 5.1 Hz, 4H, 2 × CH₂), 3.31 (s, 3H, CH₃). ¹³C NMR (151 MHz, DMSO, d₆) δ 174.81, 162.75 (¹J_{CF} = 242 Hz),

161.11, 150.05, 143.47, 142.31, 137.83 (⁴J_{CF} = 3.3 Hz), 130.66 (³J_{CF} = 8.3 Hz), 126.71, 126.44, 122.04, 121.79, 119.40, 114.55 (²J_{CF} = 24 Hz), 113.35 (²J_{CF} = 15 Hz), 112.37, 70.27, 57.63, 55.24, 37.98. HRMS (m/z, APCI) calcd for C₂₀H₁₈FN₃O₅: 400.1303 [M+1], found: 400.1324. IR (ATR) V_{max} cm⁻¹: 3239.65(N–H stretch), 3059.86(Ar–H stretch), 2930.21(C–H stretch), 1665.89(C=O stretch), 1613.55(C=O stretch).

4.2.20. 1-(3-cyanobenzyl)-N-(2-methoxyethyl)-6-nitro-4-oxo-1,4-dihydroquinolone-3-carboxamide, 23

Mustard powder, yield 55%, mp 348–350 °C. ¹H NMR (600 MHz, DMSO, d₆) δ 9.97 (t, J = 5.2 Hz, 1H, NH), 9.85 (t, J = 5.3 Hz, 1H, Ar–H), 9.27 (t, J = 3.7 Hz, 1H, Ar–H), 9.14–9.12 (m, 1H, Ar–H), 8.26 (dd, J = 9.2, 2.4 Hz, 1H, Ar–H), 7.92–7.88 (m, 1H, Ar–H), 7.84 (s, 1H, Ar–H), 7.77 (dd, J = 4.6, 3.2 Hz, 1H, Ar–H), 7.56 (dd, J = 9.2, 5.5 Hz, 1H, Ar–H), 5.90 (s, 2H, Ar–CH₂), 3.70–3.52 (m, 4H, 2 × CH₂), 3.33 (s, 3H, CH₃). ¹³C NMR (151 MHz, DMSO, d₆) δ 175.26, 175.21, 163.06, 148.77, 143.43, 139.02, 137.02, 136.84, 136.71, 130.89, 129.99, 129.71, 127.01, 121.66, 119.94, 119.81, 117.95, 70.40, 70.36, 57.62, 37.97. HRMS (m/z, APCI) calcd for C₂₁H₁₈N₄O₅: 407.1350 [M+1], found: 407.1366. IR (ATR) V_{max} cm⁻¹: 3213.77(N–H stretch), 3038.80(Ar–H stretch), 2874.49(C–H stretch), 2229.39(C≡N stretch), 1655.22(C=O stretch), 1608.88(C=O stretch).

4.2.21. 1-(4-cyanobenzyl)-N-(2-methoxyethyl)-6-nitro-4-oxo-1,4-dihydroquinolone-3-carboxamide, 24

Yellow powder, yield 60%, mp 257 °C. ¹H NMR (600 MHz, DMSO, d₆) δ 9.73 (t, J = 5.1 Hz, 1H, NH), 9.14 (s, 1H, Ar–H), 9.04 (d, J = 2.6 Hz, 1H, Ar–H), 8.50–8.40 (m, 1H, Ar–H), 7.84 (dd, J = 5.4, 8.8 Hz, 3H, Ar–H), 7.45 (t, J = 10.2 Hz, 2H, Ar–H), 5.95 (s, 2H, Ar–CH₂), 3.57–3.49 (m, 4H, 2 × CH₂), 3.32 (s, 3H, CH₃). ¹³C NMR (151 MHz, DMSO, d₆) δ 175.11, 162.91, 150.37, 143.85, 142.60, 140.90, 132.66, 127.32, 127.04, 126.71, 122.11, 119.56, 118.22, 112.90, 110.71, 70.57, 57.89, 55.67, 38.29. HRMS (m/z, APCI) calcd for C₂₁H₂₀FN₃O₆: 407.1350 [M+1], found: 407.1339. IR (ATR) V_{max} cm⁻¹: 3240.71(N–H stretch), 3056.34(Ar–H stretch), 2932.14(C–H stretch), 2227.21(C≡N stretch), 1663.15(C=O stretch), 1610.46(C=O stretch).

4.2.22. 1-(4-fluorobenzyl)-N-(2-methoxyethyl)-6-nitro-4-oxo-1,4-dihydroquinolone-3-carboxamide, 25

Yellow powder, yield 60%, mp 50 °C. ¹H NMR (600 MHz, DMSO, d₆) δ 9.78 (t, J = 5.4 Hz, 1H, NH), 9.19–9.11 (m, 1H, Ar–H), 9.02 (d, J = 2.7 Hz, 1H, Ar–H), 8.48 (dd, J = 9.4, 2.7 Hz, 1H, Ar–H), 7.98 (t, J = 9.9 Hz, 1H, Ar–H), 7.38–7.29 (m, 2H, Ar–H), 7.24–7.14 (m, 2H, Ar–H), 5.82 (s, 2H, Ar–CH₂), 3.55–3.47 (m, 4H, 2 × CH₂), 3.31 (s, 3H, CH₃). ¹³C NMR (151 MHz, DMSO, d₆) δ 175.43, 163.03 (¹J_{CF} = 243 Hz), 161.20, 150.59, 144.15, 142.96, 131.77, 129.75 (³J_{CF} = 8.3 Hz), 127.38, 127.07 (⁴J_{CF} = 3 Hz), 122.48, 120.17, 116.74 (²J_{CF} = 22 Hz), 112.99, 70.96, 58.32, 55.74, 38.66. HRMS (m/z, APCI) calcd for C₂₀H₁₈FN₃O₅: 400.1303, [M+1] found: 400.1306. IR (ATR) V_{max} cm⁻¹: 3246.88(N–H stretch), 3077.70(Ar–H stretch), 2960.02(C–H stretch), 1664.22(C=O stretch), 1613.24(C=O stretch).

4.2.23. 1-(3-cyanobenzyl)-6-nitro-4-oxo-1,4-dihydroquinolone-3-carboxylic acid, 26

Yellow powder, yield 68%, mp 265–267 °C. ¹H NMR (600 MHz, DMSO-d₆) δ 14.38 (s, 1H, COOH), 9.38 (s, 1H, Ar–H), 9.03 (s, 1H, Ar–H), 8.55 (d, J = 8.5 Hz, 1H, Ar–H), 7.97–7.53 (m, 5H, Ar–H), 5.98 (s, 2H, Ar–CH₂). ¹³C NMR (151 MHz, DMSO) δ 178.23, 165.59, 152.88, 145.00, 143.28, 137.14, 132.46, 132.01, 130.78, 130.58, 128.31, 126.53, 122.24, 120.99, 118.89, 112.40, 110.31, 56.56. HRMS (m/z, APCI) calcd for C₁₈H₁₂N₃O₅: 350.0771, [M+1] found: 350.0742.

4.3. *In vitro* antimycobacterial assay

The *In vitro* anti-tubercular evaluation was done following the procedure by Beteck et al. (2019) [39]. Briefly, a 10 mL culture of Mtb pMSP12: GFP was grown to an optical density (OD₆₀₀) of 0.6–0.7. The cultures were grown in a middlebrook 7H9 medium supplemented with 0.03% casitone, 0.4% glucose, and 0.05% tyloxapol and diluted at 1:500, prior to inoculation. The compounds to be tested were then reconstituted to a concentration of 10 mM in DMSO. Two-folds serial dilution of the test compounds were plated in 96 well plates and 50 µL of the diluted Mtb culture was then added to each well. Rifampicin (2 × MIC) was used as a minimum growth control for assay and 5% DMSO as the maximum growth control. The micro titre plates were sealed in a secondary container and incubated at 37 °C with 5% CO₂ and humidification. Fluorescence readings (excitation 485 nM; emission 520 nM) obtained for the individual wells were measured using a plate reader (FLUOstar OPTIMA, BMG LABTECH) at day 14. The raw fluorescence data was analyzed using the CDD Vault from Collaborative Drug Discovery, in which data was normalized to the minimum and maximum inhibition controls to generate a dose response curve (% inhibition). Using the Levenberg-Marquardt damped least squares method, the minimum inhibitory concentration (MIC) was calculated. The lowest concentration of drug/test compound that inhibited growth of more than 90% of the bacterial population was considered the MIC₉₀.

4.4. Docking studies

Protein crystal structure of *M. tuberculosis* DprE1 in complex with inhibitor TCA1 (PDB code: 4KW5) was obtained from the Protein Data Bank (RCSB PDB). Maestro of Schrödinger (Maestro, Schrödinger, LLC, NY, USA) was used for *in-silico* docking reported in this study. The protein crystal structure was prepared for docking using the protein preparation wizard of Glide from Schrödinger suite (Glide, Schrödinger, LLC, NY, USA), which adds the missing hydrogen atoms, assign bond orders, create zero bond orders to disulfide bonds, and delete any other heteroatoms. Glide was also used for grid generation, using the crystal ligand TCA1 as centroid of the grid box. The docked ligands were built in Marvin sketch (Marvin sketch, Schrödinger, LLC, NY, USA) and prepared for docking with LigPrep (LigPrep, Schrödinger, LLC, NY, USA). Docking was achieved with Glide ligand docking in the Maestro Package (Glide, Schrödinger, LLC, NY, USA) with default parameters settings. Docked complexes were visualized and analyzed in Maestro.

Declaration of competing interest

The authors declare that they have no known competing financial interests or personal relationships that could have appeared to influence the work reported in this paper.

Acknowledgement

PSD, L.J.L, O.J.J, R.M.B are grateful to North-West University, South Africa for financial support. The authors acknowledge the South African Medical Research Council (SHIP grant to DFW), South Africa for financial support of the anti-mycobacterial testing work. We appreciate Dr D. Otto, and Dr J. Jordaan of Chemical Resource Beneficiation unit, Potchefstroom, South Africa for generation of NMR and HRMS data. *M. ulcerans* susceptibility testing was done by Prof. Gerd Pluschke, Switzerland.

Appendix A. Supplementary data

Supplementary data to this article can be found online at <https://doi.org/10.1016/j.ejmech.2021.113207>.

Data availability statement

Dose-response curves and characterization data (¹H, ¹³C and HRMS spectra) for compounds **3a**, and **5–26** are available in the supplementary file. Samples of compounds can be obtained from corresponding author upon reasonable request.

References

- [1] B.A. Forbes, *Mycobacterial taxonomy*, *J. Clin. Microbiol.* 55 (2017) 380–383.
- [2] R.V. Chikhale, M.A. Barmade, P.R. Murumkar, M.R. Yadav, Overview of the development of dprE1 inhibitors for combating the menace of tuberculosis, *J. Med. Chem.* 61 (2018) 8563–8593.
- [3] R. Koch, *Die ätiologie der Tuberkulose*, *Berliner Klinische Wschr* 19 (1882) 221–230.
- [4] WHO, The Who Global Task Force on TB Impact Measurement, World Health Organization, 2019. Accessed from https://www.who.int/tb/areas-of-work/monitoring-evaluation/impact_measurement_taskforce/en/on_26/10/2020.
- [5] G. Churchyard, P. Kim, N.S. Shah, R. Rustonjee, N. Gandhi, B. Mathema, D. Dowdy, A. Kasmar, et al., What we know about tuberculosis transmission: an overview, *J. Infect. Dis.* 216 (2017) S629–S635.
- [6] K.S. Cho, Tuberculosis control in the Republic of Korea, *Epidemiol. Health* 40 (2018) e2018036.
- [7] N.S. Shah, S.C. Auld, J.C. Brust, B. Mathema, N. Ismail, P. Moodley, K. Mlisana, S. Allana, Transmission of extensively drug-resistant tuberculosis in South Africa. *N. Engl. J. Med.* 376 (2017) 243–253.
- [8] M.M. Islam, H.M. Hameed, J. Mugweru, C. Chhotaray, C. Wang, Y. Tan, J. Liu, X. Li, et al., Drug resistance mechanisms and novel drug targets for tuberculosis therapy, *J. Genet. Genomics* 44 (2017) 21–37.
- [9] D. Sharma, B. Kumar, M. Lata, B. Joshi, K. Venkatesan, S. Shukla, D. Bisht, Comparative proteomic analysis of aminoglycosides resistant and susceptible mycobacterium tuberculosis clinical isolates for exploring potential drug targets, *PLoS One* 10 (2015) e0139414.
- [10] S. Tiberi, M. Munoz-Torrico, R. Duarte, M. Dalcolmo, L. D'Ambrosio, G.B. Migliori, New drugs and perspectives for new anti-tuberculosis regimens, *Pulmonology* 24 (2018) 86–98.
- [11] M.G. Kale, A.P. Raichurkar, D. Waterson, D. McKinney, M.R. Manjunatha, U. Kranthi, K. Koushik, et al., Thiazolopyridine ureas as novel antitubercular agents acting through inhibition of DNA gyrase B, *J. Med. Chem.* 56 (2013) 8834–8848.
- [12] K. Nepali, H.-Y. Lee, J.-P. Liou, Nitro-group-containing drugs, *J. Med. Chem.* 6 (2019) 2851–2893.
- [13] T. Christophe, M. Jackson, H.K. Jeon, D. Fenistein, M. Contreras-Dominguez, J. Kim, A. Genovesio, J.-P. Carralot, et al., High content screening identifies decaprenyl-phosphoribose 2' epimerase as a target for intracellular antimycobacterial inhibitors, *PLoS Pathog.* 5 (2009) e1000645.
- [14] M. Brečič, I. Centárová, R. Mukherjee, G.I. Kolly, S. Huszár, A. Bobovská, E.K. Kilacksová, V. Mokosová, et al., DprE1 is a vulnerable tuberculosis drug target due to its cell wall localization, *ACS Chem. Biol.* 10 (2015) 1631–1636.
- [15] K. Mikusova, V. Makarov, J. Neres, DprE1—from the discovery to the promising tuberculosis drug target, *Curr. Pharmaceut. Des.* 20 (2014) 4379–4403.
- [16] V. Makarov, B. Lechartier, M. Zhang, J. Neres, A.M. van der Sar, S.A. Raadsen, R.C. Hartkoorn, O.B. Ryabova, et al., Towards a new combination therapy for tuberculosis with next generation benzothiazinones, *EMBO Mol. Med.* 6 (2014) 372–383.
- [17] P.S. Shirude, P. Madhavapeddi, J.A. Tucker, K. Murugan, V. Patil, H. Basavarajappa, A.V. Raichurkar, V. Humnabardkar, et al., Aminopyrazinamides: novel and specific gyrB inhibitors that kill replicating and nonreplicating mycobacterium tuberculosis, *ACS Chem. Biol.* 8 (2013) 519–523.
- [18] P.K. Crellin, R. Brammananth, R.L. Coppel, Decaprenylphosphoryl-β-d-ribose 2'-epimerase, the target of benzothiazinones and dinitrobenzamides, is an essential enzyme in mycobacterium smegmatis, *PLoS One* 6 (2011) e16869.
- [19] S. Magnet, R.C. Hartkoorn, R. Székely, J. Pató, J.A. Triccas, P. Schneider, C. Szántai-Kis, L. Órfi, et al., Leads for antitubercular compounds from kinase inhibitor library screens, *Tuberculosis* 90 (2010) 354–360.
- [20] C. Trefzer, M. Rengifo-Gonzalez, M.J. Hinner, P. Schneider, V. Makarov, S.T. Cole, K. Johnsson, Benzothiazinones: prodrugs that covalently modify the decaprenylphosphoryl-β-d-ribose 2'-epimerase dprE1 of mycobacterium tuberculosis, *J. Am. Chem. Soc.* 132 (2010) 13663–13665.
- [21] J. Roh, G. Karabanovich, H. Vlčková, A. Carazo, J. Němeček, P. Sychra, L. Valášková, O. Pavliš, et al., Development of water-soluble 3, 5-dinitrophenyl tetrazole and oxadiazole antitubercular agents, *Bioorg. Med. Chem.* 25 (2017) 5468–5476.
- [22] K.N. Venugopala, S. Chandrashekarappa, M. Pillay, S. Bhandary, M. Kandeel,

- F.M. Mahomoodally, M.A. Morsy, D. Chopra, et al., Synthesis and structural elucidation of novel benzothiazole derivatives as anti-tubercular agents: in-silico screening for possible target identification, *Med. Chem.* 15 (2019) 311–326.
- [23] M. Gjorgjieva, T. Tomašič, D. Kikelj, L. Mašič, Benzothiazole-based compounds in antibacterial drug discovery, *Curr. Med. Chem.* 25 (2018) 5218–5236.
- [24] G. Riccardi, M.R. Pasca, L.R. Chiarelli, G. Manina, A. Mattevi, C. Binda, The dpre1 enzyme, one of the most vulnerable targets of mycobacterium tuberculosis, *Appl. Microbiol. Biotechnol.* 97 (2013) 8841–8848.
- [25] R. Zhang, B. K Lv, L. Wang, B. Li, M. Wang, H. Liu, A. Guo, Wang, Design, synthesis and antitubercular evaluation of benzothiazinones containing an oximido or amino nitrogen heterocycle moiety, *RSC Adv.* 7 (2017) 1480–1483.
- [26] J. Shi, J. Lu, Z. Zong, F. Huo, J. Luo, Q. Liang, Y. Li, H. Huang, In vitro activity of pbtz169 against multiple mycobacterium species, *Antimicrob. Agents Chemother.* 62 (2018) e01314–e01318.
- [27] V. Makarov, K. Mikušová, Development of Macozinone for TB treatment: An Update, *Appl. Sci.* 10 (2020) 2269.
- [28] S. Keshavjee, P.E. Farmer, Tuberculosis, drug resistance, and the history of modern medicine, *N. Engl. J. Med.* 367 (2012) 931–936.
- [29] S.B. Marganakop, R.R. Kamble, T. Taj, M.Y. Kariduraganvar, An efficient one-pot cyclization of quinoline thiosemicarbazones to quinolines derivatized with 1, 3, 4-thiadiazole as anticancer and anti-tubercular agents, *Med. Chem. Res.* 21 (2012) 185–191.
- [30] K.K. Kumar, S.P. Seenivasan, V. Kumar, T.M. Das, Synthesis of quinoline coupled [1, 2, 3]-triazoles as a promising class of anti-tuberculosis agents, *Carbohydr. Res.* 346 (2011) 2084–2090.
- [31] A. Marella, O.P. Tanwar, R. Saha, M.R. Ali, S. Srivastava, M. Akhter, M. Shaquiquzzaman, M.M. Alam, Quinoline: a versatile heterocyclic. *Saudi. Pharm. J.* 21 (2013) 1–12.
- [32] R.M. Beteck, A. Jordaan, T. Swart, F. Van der Kooy, D.F. Warner, H.C. Hoppe, L.J. Legoabe, 6-Nitro-1-benzylquinolones exhibiting specific antitubercular activity, *Chem. Biol. Drug. DES* (2020) 1–8, 00.
- [33] N. Scherr, G. Pluschke, M. Panda, Comparative study of activities of a diverse set of antimycobacterial agents against *Mycobacterium tuberculosis* and *Mycobacterium ulcerans*, *Antimicrob. Agents Chemother.* 60 (2016) 3132–3137.
- [34] G. Karabanovich, J. Dusek, K. Savkova, O. Pavlis, I. Pávkova, Development of 3,5-dinitrophenyl-containing 1,2,4-triazoles and their trifluoromethyl analogues as highly efficient antitubercular agents inhibiting Decaprenylphosphoryl- β -D-ribofuranose 2'-oxidase, *ACS Med. Chem.* 62 (2019) 8115–8139.
- [35] K.D. Freeman-Cook, R.L. Hoffman, T.W. Johnson, Lipophilic efficiency: the most important efficiency metric in medicinal chemistry, *Future Med. Chem.* 5 (2013) 113–115.
- [36] C.A. Lipinski, Lead-and drug-like compounds: the rule-of-five revolution, *Drug. Discov. Today, Technol.* 1 (2004) 337–341.
- [37] S.D. Krämer, H.E. Aschmann, M. Hatibovic, K.F. Hermann, C.S. Neuhaus, C. Brunner, S. Belli, When barriers ignore the "rule-of-five", *Adv. Drug Deliv. Rev.* 101 (2016) 62–74.
- [38] R.M. Beteck, R. Seldon, A. Jordaan, D.F. Warner, H.C. Hoppe, D. Laming, S.D. Khanye, New quinolone-based thiosemicarbazones showing activity against *Plasmodium falciparum* and *Mycobacterium tuberculosis*, *Molecules* 9 (2019) 24.
- [39] R.M. Beteck, R. Seldon, A. Jordaan, D.F. Warner, H.C. Hoppe, D. Laming, L.J. Legoabe, S.D. Khanye, Quinolone-isoniazid hybrids: synthesis and preliminary in vitro cytotoxicity and anti-tuberculosis evaluation, *Med. Chem. Commun* 10 (2019) 326–331.